

Signatures of quantum stability in a classically chaotic system

S. Schlunk,¹ M.B. d’Arcy,¹ S.A. Gardiner,¹ D. Cassettari,¹ R.M. Godun,¹ and G.S. Summy^{1,2}

¹Clarendon Laboratory, Department of Physics, University of Oxford, Parks Road, Oxford, OX1 3PU, United Kingdom

²Department of Physics, Oklahoma State University, Stillwater, Oklahoma, 74078-3072

(Dated: November 9, 2018)

We experimentally and numerically investigate the quantum accelerator mode dynamics of an atom optical realization of the quantum δ -kicked accelerator, whose classical dynamics are chaotic. Using a Ramsey-type experiment, we observe interference, demonstrating that quantum accelerator modes are formed coherently. We construct a link between the behavior of the evolution’s fidelity and the phase space structure of a recently proposed pseudoclassical map, and thus account for the observed interference visibilities.

PACS numbers: 05.45.Mt, 03.65.Sq, 32.80.Lg, 42.50.Vk

The relationship between the behaviour of classical and quantum systems, and how macroscopic classical phenomena originate in the quantum regime, remain subjects of dispute [1]. The issues involved are particularly marked for quantum versions of classically chaotic systems [2]. Experimental investigations of such systems began with studies of microwave-driven hydrogen [3]; subsequent work has also centred on microwave cavities [4], mesoscopic solid-state systems [5], and atom optics [6], the approach we adopt. In this Letter we consider the quantum δ -kicked accelerator [7, 8, 9], a δ -kicked rotor with an additional static linear potential. The δ -kicked rotor is one of the most extensively investigated systems in chaotic dynamics [10], and is equivalent to a free particle subjected periodically to instantaneous momentum kicks from a sinusoidal potential. Quantum mechanically, the effect of these kicks is to diffract the particles’ constituent de Broglie waves into a series of discrete momentum states. In the δ -kicked accelerator, the linear potential modifies the chaotic classical dynamics only slightly, yet can radically change the quantum behaviour. The phases accumulated between consecutive kicks by the momentum states are altered, leading to the creation of quantum accelerator modes [7, 8, 9]. We realize quantum δ -kicked accelerator dynamics in laser-cooled cesium atoms by the application of short pulses of a vertical standing wave of off-resonant laser light, which constitutes a sinusoidal potential; gravity provides the linear potential. Quantum accelerator modes, absent in the analogous classical dynamics, are observed and are characterized by a linear (with kick number) momentum transfer to a substantial fraction ($\sim 20\%$) of the atoms. If coherent, this efficient momentum transfer promises applications in atom interferometry [11]. In this Letter we use a Ramsey-type interference experiment [12] to show that quantum accelerator modes do preserve coherence. We then relate the Ramsey fringe contrast to the fidelity f [13]; by a numerical analysis, we link the behaviour of f to the phase space structure of the δ -kicked accelerator in a pseudoclassical limit recently proposed by Fishman *et al.* [14]. Finally we explain differences in the observed fringe visibilities by examining the effect of the experimental range of kicking strengths.

In our interference experiment, the atoms undergo δ -kicked accelerator dynamics, between the application of two $\pi/2$ mi-

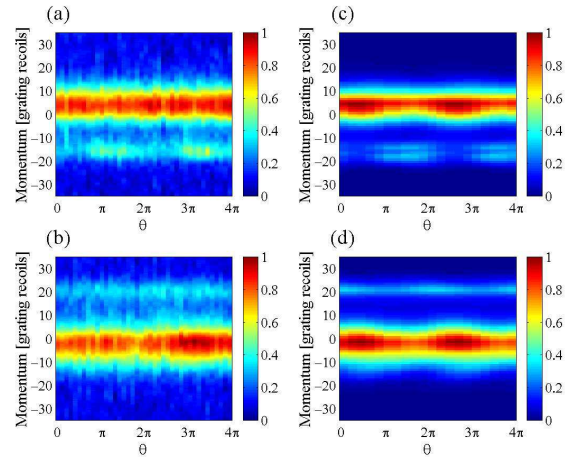


FIG. 1: Experimentally measured momentum distributions as the microwave phase difference θ is varied in a $\pi/2$ — 20 kick — $\pi/2$ sequence where $\delta_L^b \sim 35$ GHz, with (a) $T = 60.5\mu\text{s}$ (accelerator mode at $-17\hbar G$), and (b) $T = 74.5\mu\text{s}$ (accelerator mode at $20\hbar G$). The corresponding numerically generated momentum distributions, where $\delta_L^b = 35$ GHz, are shown in (c) and (d). Population has been arbitrarily normalized to maximum value = 1.

crowave pulses that couple two atomic hyperfine levels. In the absence of coherence-destroying spontaneous emission, the contrast of any interference fringes is related to the overlap of two initially identical motional states evolved under the influence of slightly different Hamiltonians [15], i.e. the fidelity. It can therefore yield information on the sensitivity of the atoms’ evolution to variations in the kicking strength. Strong sensitivity can be considered a quantum signature of chaos, particularly in the semiclassical limit ($\hbar \rightarrow 0$), hence the use by Peres [16] of f as a measure of quantum stability.

After magneto-optic trapping and molasses cooling to $5\mu\text{K}$, we prepare around 10^6 freely falling cesium atoms in the $F = 3, m_F = 0$ hyperfine level (denoted $|a\rangle$) of the $6^2\text{S}_{1/2}$ ground state [17]. The first $\pi/2$ microwave pulse creates an equal superposition of the atoms’ internal states, i.e., $|a\rangle \rightarrow (|a\rangle - ie^{i\theta}|b\rangle)/\sqrt{2}$, where $|b\rangle$ denotes the $F = 4, m_F = 0$ level. The phase θ of this pulse can be changed with respect

to that of the second $\pi/2$ pulse, applied following 20 equally spaced 500 ns pulses from a standing wave of light. This is formed by retroreflection of a Ti:sapphire laser beam; its maximum intensity is $\sim 1 \times 10^8$ mW/cm² [9], and the light is red-detuned by 45 and 35 GHz from the D1 transition for atoms in states $|a\rangle$ and $|b\rangle$, respectively. After the second $\pi/2$ microwave pulse, we measure the momentum distribution in state $|b\rangle$ by a time-of-flight method. For more details of our experimental setup see Refs. [8, 9]. Measurement of a periodic variation with θ in the accelerator mode population in state $|b\rangle$, i.e. interference, directly implies coherent evolution.

In the limit of large detuning, the Hamiltonian is

$$\hat{H} = \hat{H}_a|a\rangle\langle a| + \hat{H}_b|b\rangle\langle b| + \frac{\hbar\omega_{ab}}{2}(|b\rangle\langle b| - |a\rangle\langle a|), \quad (1)$$

where $\hbar\omega_{ab}$ is the energy gap between $|a\rangle$ and $|b\rangle$, and

$$\hat{H}_\sigma = \frac{\hat{p}^2}{2m} + mg\hat{z} - \frac{\hbar\Omega^2 t_p}{8\delta_L^\sigma} [1 + \cos(G\hat{z})] \sum_n \delta(t - nT) \quad (2)$$

is the quantum δ -kicked accelerator Hamiltonian, acting on atoms in internal state $|\sigma\rangle \in \{|a\rangle, |b\rangle\}$. Here \hat{z} is the vertical position, \hat{p} the z -direction momentum, m the particle mass, g the gravitational acceleration, t the time, T the pulsing period, Ω the Rabi frequency, t_p the pulse duration, δ_L^σ the detuning from the D1 transition for the state $|\sigma\rangle$, and $G = 4\pi/\lambda$, where $\lambda = 894$ nm is the laser wavelength, and $\hbar G$ is a grating recoil (the momentum separation of adjacent diffracted states). We denote the amplitude of the phase modulation to atoms in state $|b\rangle$ that results from application of the standing wave as $\phi_d = \Omega^2 t_p / 8\delta_L^b$. The experimental mean value of ϕ_d is 0.8π , and, due to the different detuning, that of the corresponding quantity for atoms in state $|a\rangle$ is $\phi_d^a = \phi_d \delta_L^b / \delta_L^a = 0.6\pi$. We thus have effectively two different Hamiltonians, applied to the same initial motional state. The pulse train leads to the creation of a quantum accelerator mode, the momentum of which is the same for the two internal states [8]. We consider pulse periods $T = 60.5\mu\text{s}$ and $74.5\mu\text{s}$, close to $T_{1/2} = 2\pi m / \hbar G^2 = 66.7\mu\text{s}$, which corresponds to the lowest second-order quantum resonance in the δ -kicked rotor [9, 18]. For these T , well-populated accelerator modes involving substantial momentum transfer are created [7, 8, 9].

Figure 1(a) shows the measured final momentum distributions of $|b\rangle$ atoms, for $T = 60.5\mu\text{s}$. We see a period- 2π variation with θ in the accelerator mode population (at around $-17\hbar G$), the visibility V of which is $(21 \pm 2)\%$ [20]. We observe similar fringes for a range of detunings ($\delta_L^b = 20$ – 40 GHz) and total number of kicks $N = 10$ – 30 . However, depending on their exact values, V can vary between 10% and 40%. This periodic variation of the population demonstrates interference, and hence that the accelerator mode transfers momentum coherently. At $T = 74.5\mu\text{s}$ [Fig. 1(b)], however, fringes in the accelerator mode (at around $20\hbar G$) are practically invisible, despite the expected coherent nature of the momentum transfer. In Figs. 1(c) and 1(d) diffraction-based numerical simulations [7, 8, 9], incorporating the experimental range of ϕ_d (0.3π to 1.2π), also show this difference in the

fringe visibility for the two values of T . The range of ϕ_d is due to the Gaussian profile of the standing wave intensity (FWHM ~ 1 mm) and the spatial extent of the atomic cloud (Gaussian density distribution, FWHM ~ 1 mm) [9]. As we optimized the overlap of the laser beams with the atomic cloud, the intensity and density maxima can be assumed to be coincident. The calculated visibility is then 25% for $T = 60.5\mu\text{s}$ [Fig. 1(c)] but only 8% for $T = 74.5\mu\text{s}$ [Fig. 1(d)].

In order to explain these surprising observations, we introduce the Floquet operator $\hat{F}_b(\phi_d)$. This describes the effect of one kick and the subsequent free evolution on the motional state of atoms in state $|b\rangle$, where

$$\hat{F}_b(\phi_d) = \exp(-i[\gamma\hat{\chi} + \hat{\rho}^2/2]/\hbar) \exp(i\phi_d[1 + \cos\hat{\chi}]). \quad (3)$$

We define $\hat{F}_a(\phi_d)$ analogously for state $|a\rangle$, with ϕ_d replaced by ϕ_d^a [19]. As in Ref. [9], we use scaled position and momentum variables $\chi = Gz$ and $\rho = GTp/m$, while $\gamma = gGT^2$ describes the effect of gravity, and $\hbar = \hbar G^2 T / m = -i[\hat{\chi}, \hat{\rho}]$ is an effective scaled Planck constant. After N pulses an initial plane wave $|q\rangle$ of wavenumber q evolves to $\hat{F}_\sigma(\phi_d)^N |q\rangle = e^{i\phi_d N} |\psi_\sigma^q(\phi_d)\rangle$, where $\phi = \phi_d$ or ϕ_d^a , as appropriate. Regarding the initial motional state as an incoherent superposition of $|q\rangle$, the momentum distribution in state $|b\rangle$ for a given ϕ_d after the $\pi/2 - N$ kick $- \pi/2$ sequence, is

$$P_b(\phi_d, p) = \frac{1}{4} \int dq C(q) [|\psi_a^q(\phi_d, p)|^2 + |\psi_b^q(\phi_d, p)|^2] + \frac{1}{2} \left| \int dq C(q) \psi_a^q(\phi_d, p)^* \psi_b^q(\phi_d, p) \right| \times \cos(\phi_I(\phi_d, p) + N\delta\phi_d + \theta), \quad (4)$$

where $\delta\phi_d = \phi_d - \phi_d^a$, $\psi_\sigma^q(\phi_d, p) = \langle p | \psi_\sigma^q(\phi_d) \rangle$, and ϕ_I is the phase of the interference term, i.e., $\int dq C(q) \psi_a^q \psi_b^{q*} = |\int dq C(q) \psi_a^q \psi_b^{q*}| e^{i\phi_I}$. The weighting $C(q)$ describes the initial Gaussian momentum distribution (FWHM = 6 grating recoils $\hbar G$). The third (interference) term in Eq. (4) is responsible for the appearance of fringes in the accelerated $|b\rangle$ population. We denote the amplitude of the modulation in P_b by $A(\phi_d, p)/2 = |\int dq C(q) \psi_a^q(\phi_d, p)^* \psi_b^q(\phi_d, p)|/2$, where $\int dp A(\phi_d, p)^2 = f(\phi_d)$ is the fidelity for a given ϕ_d .

We have calculated the individual terms of P_b numerically for a wide range of ϕ_d , obtaining as a consequence an important result linking the pseudoclassical analysis of Fishman *et al.* [14] with the quantum stability measure of Peres [16]. Comparison of Figs. 2(a) and 2(c) with Fig. 1 shows that the region in momentum space corresponding to an accelerator mode is also a region of high A . This remains high up to large values of ϕ_d [21], continuing beyond the point at which it has decayed to nearly zero in other regions of momentum space. As $f = \int dp A^2$, its large value when determined by integrating over the momenta populated by atoms in the quantum accelerator mode implies that these atoms inhabit a stable region of quantum state space. Note that small A does not necessarily imply low atomic population, as can be seen in the plots of the non-interfering population $\int dq C(q) (|\psi_a^q|^2 + |\psi_b^q|^2)/4$ in Figs. 2(b) and 2(d). Contrasting Fig. 2(a) with Fig. 2(c), we

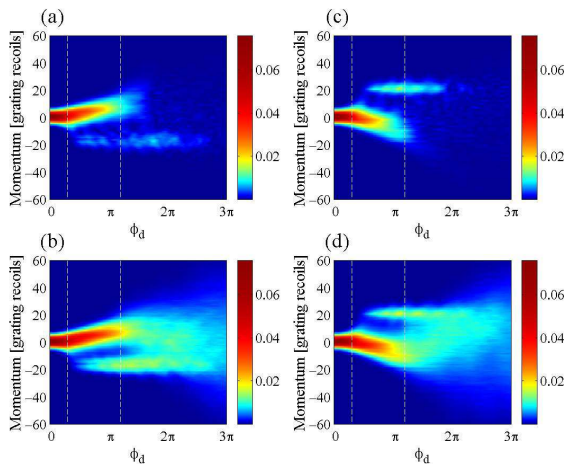


FIG. 2: Plots of $A/2$ against ϕ_d with $N = 20$, for (a) $T = 60.5\mu\text{s}$ and (c) $T = 74.5\mu\text{s}$. Plots of the non-interfering population $\int dq C(q)(|\psi_a^q|^2 + |\psi_b^q|^2)/4$ for (b) $T = 60.5\mu\text{s}$ and (d) $T = 74.5\mu\text{s}$. Dashes mark the boundaries of the experimental range. Accelerator modes exist at $-17\hbar G$ for (a) and (c), and at $20\hbar G$ for (b) and (d).

see that this large value of A extends over a significantly wider range of ϕ_d for $T = 60.5\mu\text{s}$ than for $T = 74.5\mu\text{s}$. Hence, we can interpret the accelerator mode at $T = 60.5\mu\text{s}$ as being more robust to variations in ϕ_d , i.e. more *stable*, compared with that at $T = 74.5\mu\text{s}$. However given our comparatively narrow experimental range of ϕ_d , this does not explain the difference in fringe visibilities seen in Fig. 1.

The appearance of quantum accelerator modes in the δ -kicked accelerator is explained in the analysis of Fishman *et al.* [14] in terms of islands of stability centred on stable fixed points in the phase space generated by the map [22]:

$$\tilde{\rho}_{n+1} = \tilde{\rho}_n - \tilde{k} \sin(\chi_n) - \text{sign}(\epsilon)\gamma, \quad (5)$$

$$\chi_{n+1} = \chi_n + \text{sign}(\epsilon)\tilde{\rho}_{n+1}, \quad (6)$$

where the population of a mode is proportional to the size of the corresponding island. This is a *pseudoclassical* [$\epsilon = (\tilde{k} - 2\pi) \rightarrow 0$] rather than *semiclassical* ($\tilde{k} \rightarrow 0$) limit of the quantum dynamics characterized by the Floquet operator of Eq. (3). We have introduced $\tilde{\rho} = \rho\epsilon/\tilde{k}$ (in an accelerating frame [14]) and $\tilde{k} = \phi_d|\epsilon|$. Classically, the system is globally chaotic for our parameter regime. Figure 3 shows the pseudoclassical phase spaces generated by iteration of Eqs. (5) and (6) for the experimentally investigated values of $\epsilon = 2\pi(T/T_{1/2} - 1)$, and a range of ϕ_d . When $\phi_d = 0.3\pi$ [Figs. 3(a) and 3(d)], the island (based around a stable fixed point in phase space) is substantially smaller for $T = 74.5\mu\text{s}$ than for $T = 60.5\mu\text{s}$. For the average experimental value of ϕ_d (0.8π) [Figs. 3(b) and 3(e)], the islands have both grown to be about the same size. For $\phi_d = 1.5\pi$ [Figs. 3(c) and 3(f)], the island has shrunk dramatically in the case of $T = 74.5\mu\text{s}$, while at $T = 60.5\mu\text{s}$ the island has also shrunk, but not to the same extent. We therefore conclude that the stable island representing the accelerator mode

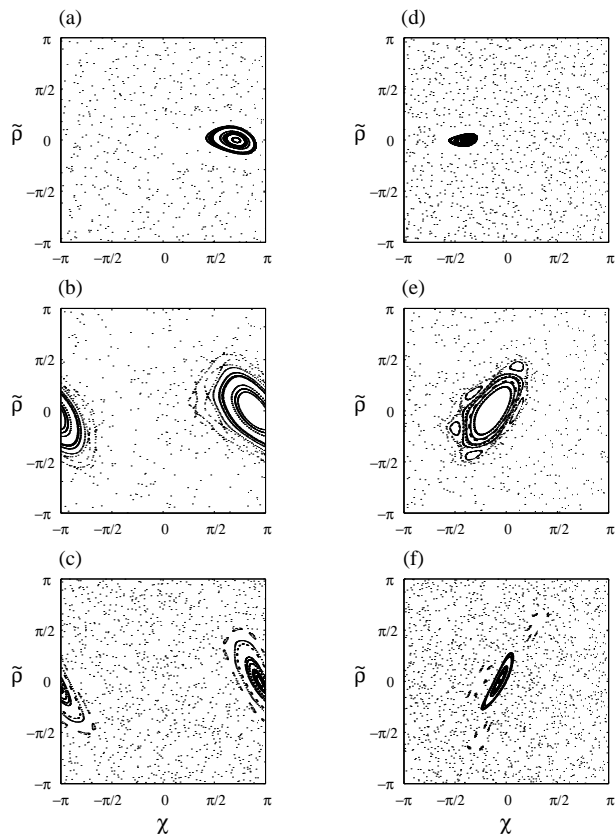


FIG. 3: Stroboscopic pseudoclassical Poincaré sections determined by Eqs. (5) and (6) for $T = 60.5\mu\text{s}$ ($\Rightarrow \epsilon = -0.58$), and for (a) $\phi_d = 0.35\pi$, (b) the average experimental value 0.8π , and (c) 1.5π . Figures (d), (e), and (f) show corresponding plots for $T = 74.5\mu\text{s}$ ($\Rightarrow \epsilon = 0.73$). Displayed units are dimensionless.

is much more robust to perturbations in the kicking strength for $T = 60.5\mu\text{s}$ than for $T = 74.5\mu\text{s}$. The fact that A (and therefore f) remains large at the accelerator mode momentum for a significantly broader range of ϕ_d when $T = 60.5\mu\text{s}$ than for when $T = 74.5\mu\text{s}$, as shown in Fig. 2, matches exactly the observed greater stability of the island in the pseudoclassical phase space for $T = 60.5\mu\text{s}$. This is consistent with Peres's identification of the behaviour of the fidelity as reflecting stability properties of the phase space in the semiclassical limit [16], even though our experiment (and numerics) operate in a pseudoclassical regime which is far from semiclassical.

The position of the islands in pseudoclassical phase space in Fig. 3 indicates the region of the quantum accelerator modes' spatial localization. For $T = 60.5\mu\text{s}$ this is where there is zero standing light wave intensity, whereas when $T = 74.5\mu\text{s}$, it is where the intensity, and hence phase shift, are maximal [23]. We thus expect the modulation of the P_b interference term in Eq. (4), $\cos(\phi_I + N\delta\phi_d + \theta)$, to have a strong dependence on ϕ_d for the momenta at which accelerator modes are found when $T = 74.5\mu\text{s}$, but not when $T = 60.5\mu\text{s}$. This is confirmed by Figs. 4(a) and 4(b), where $\cos(\phi_I + N\delta\phi_d + \theta)$

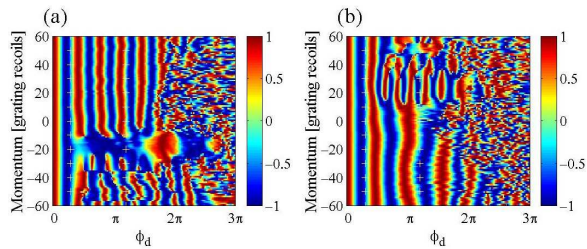


FIG. 4: Plots of $\cos(\phi_I + N\delta\phi_d)$ against ϕ_d with $N = 20$, for (a) $T = 60.5\mu\text{s}$ and (b) $T = 74.5\mu\text{s}$. Crosses mark the boundaries of the experimental range.

is plotted as a function of p and ϕ_d for constant θ (set to 0 for convenience) for $T = 60.5\mu\text{s}$ and $T = 74.5\mu\text{s}$, respectively. At the accelerator mode momentum, the value of $\cos(\phi_I + N\delta\phi_d)$ at $T = 60.5\mu\text{s}$ is almost independent of ϕ_d , whereas at $T = 74.5\mu\text{s}$ there is an approximate frequency doubling, relative to other momenta. We can now explain the presence or absence of interference fringes in Fig. 1 in terms of this difference in ϕ_d dependence. As Eq. (4) determines the population for one specific value of ϕ_d only, the observable momentum distribution is $\bar{P}_b(p) = \int d\phi_d D(\phi_d) P_b(\phi_d, p)$, where $D(\phi_d)$ is a distribution describing the proportion of atoms experiencing a particular ϕ_d . Although for a single value of ϕ_d the visibility of the fringes at both $T = 60.5\mu\text{s}$ and $T = 74.5\mu\text{s}$ is high, Figs. 4(a) and 4(b) show that integration over the experimental range of ϕ_d causes a greater reduction in visibility at $T = 74.5\mu\text{s}$ than at $T = 60.5\mu\text{s}$. At large ϕ_d (greater than occurs in our experiment), there is a breakdown of all structure in plots of $\cos(\phi_I + N\delta\phi_d)$. Comparing with Figs. 2(a) and 2(c), we observe this to coincide with a falloff in A . Note, however, that as ϕ_I is determined numerically from complex interference terms, one should be careful about attaching significance to values of $\cos(\phi_I + N\delta\phi_d)$ for which the corresponding value of A is close to zero.

In summary, we have performed a Ramsey-type interference experiment and thus demonstrated the coherence of the production of quantum accelerator modes, and hence their suitability for applications in atom interferometry. Numerically, we have found the accelerator modes to correspond to regions of greater quantum stability, as quantified by the fidelity. This is consistent with the presence of stable regions in the phase space of a recently proposed pseudoclassical limit of δ -kicked accelerator dynamics, rather than the globally chaotic behaviour of the semiclassical limit. These regions dictate the position of the accelerator modes' spatial localization, allowing us to explain the lack of fringes for the accelerator mode at certain pulse periods, due to the experimental range of kicking strengths. Our investigation of coherence in quantum accelerator modes has allowed observation of their quantum-stable dynamics in this classically chaotic system.

We thank R. Bach, K. Burnett, S. Fishman, I. Guarneri, L.

Rebuzzini, and S. Wimberger for stimulating discussions. We acknowledge support from the UK EPSRC, the Paul Instrument Fund of The Royal Society, the EU through the TMR 'Cold Quantum Gases' network (contract no. HPRN-CT-2000-00125) and the Marie Curie fellowship program (D.C.), the DAAD (S.S.), the Royal Commission for the Exhibition of 1851 (M.B.d'A.), and Christ Church, Oxford (R.M.G.)

-
- [1] W.H. Zurek, *Phys. Today* **44**, (10) 36 (1991).
 - [2] F. Haake, *Quantum Signatures of Chaos* (2nd ed.) (Springer-Verlag, Berlin, 2001); *New Directions in Quantum Chaos*, edited by G. Casati *et al.*, (IOS Press, Amsterdam, 2000).
 - [3] J.E. Bayfield *et al.*, *Phys. Rev. Lett.* **63**, 364 (1989); M. Arndt *et al.*, *ibid.* **67**, 2435 (1991); P.M. Koch and K.A.H. van Leeuwen, *Phys. Rep.* **255**, 289 (1995).
 - [4] S. Sridhar and E.J. Heller, *Phys. Rev. A* **46** R1728 (1992); A. Kudrolli *et al.*, *Phys. Rev. E* **49** R11 (1994).
 - [5] P.B. Wilkinson *et al.*, *Nature (London)* **380**, 608 (1996); J.P. Bird *et al.*, *Phys. Rev. Lett.* **82**, 4691 (1999); P.B. Wilkinson *et al.*, *ibid.* **86**, 5466 (2001).
 - [6] F.L. Moore *et al.*, *Phys. Rev. Lett.* **75**, 4598 (1995); B.G. Klappauf *et al.*, *ibid.* **81**, 1203 (1998); H. Ammann *et al.*, *ibid.* **80**, 4111 (1998); W.K. Hensinger *et al.*, *Nature (London)* **412**, 52 (2001); D.A. Steck *et al.*, *Science* **293**, 274 (2001).
 - [7] M.K. Oberthaler *et al.*, *Phys. Rev. Lett.* **83**, 4447 (1999).
 - [8] R.M. Godun *et al.*, *Phys. Rev. A* **62**, 013411 (2000).
 - [9] M.B. d'Arcy *et al.*, *Phys. Rev. E* **64**, 056233 (2001).
 - [10] A.L. Lichtenberg and M.A. Lieberman, *Regular and Chaotic Dynamics* (Springer-Verlag, Berlin, 1992); G. Casati *et al.*, in *Stochastic Behavior in Classical and Quantum Hamiltonian Systems*, (Springer-Verlag, New York, 1979).
 - [11] P. Berman, *Atom Interferometry* (Academic Press, San Diego, 1997).
 - [12] *Molecular Beams*, edited by N.F. Ramsey (Oxford University Press, Oxford, 1986).
 - [13] G. Benenti and G. Casati, *Phys. Rev. E* **65** 066205 (2002).
 - [14] S. Fishman *et al.*, *Phys. Rev. Lett.* **89**, 084101 (2002), and e-print nlin.CD/0202047.
 - [15] S.A. Gardiner *et al.*, *Phys. Rev. Lett.* **79**, 4790 (1997).
 - [16] A. Peres, *Quantum Theory: Concepts and Methods* (Kluwer Academic Publishers, Dordrecht, 1993). See, also, R. Schack and C.M. Caves, *Phys. Rev. E* **53**, 3257 and 3387 (1996); G. Garcia de Polavieja, *Phys. Rev. A*, **57**, 3184 (1998).
 - [17] Here F is the total electronic plus nuclear angular momentum, and m_F is the projection on the quantization axis.
 - [18] W.H. Oskay *et al.*, *Opt. Commun.* **179**, 137 (2000); M.B. d'Arcy *et al.*, *Phys. Rev. Lett.* **87**, 074102 (2001).
 - [19] As ϕ_d^a is determined by ϕ_d , \hat{F}_a is written as a function of ϕ_d .
 - [20] We define the visibility by $V = (S_{\max} - S_{\min}) / (S_{\max} + S_{\min})$, where S is the accelerator mode population in state $|b\rangle$.
 - [21] Note that $\delta\phi_d = \phi_d(1 - \delta_L^b / \delta_L^a)$ grows linearly with ϕ_d . Thus, as ϕ_d increases, so does the difference between \hat{H}_a and \hat{H}_b .
 - [22] Here χ_n and $\tilde{\rho}_n$ specify χ and $\tilde{\rho}$ just prior to kick $n + 1$, rather than just after kick n , as in Ref. [14].
 - [23] This is consistent with fully quantum numerics described by M.B. d'Arcy, *Quantum Chaos in Atom Optics*, D. Phil. thesis (University of Oxford, 2002).